Title

Monitoring acute metabolic changes in the liver and kidneys induced by fructose and glucose using hyperpolarized [2-13C]dihydroxyacetone

Journal

Magnetic Resonance in Medicine, 77(1)

ISSN

0740-3194

Authors

Marco-Rius, Irene

von Morze, Cornelius

Sriram, Renuka

et al.

Publication Date

2017

DOI

10.1002/mrm.26525

Peer reviewed

HHS Public Access

Author manuscript

Magn Reson Med. Author manuscript; available in PMC 2018 January 01.

Published in final edited form as:

Magn Reson Med. 2017 January ; 77(1): 65–73. doi:10.1002/mrm.26525.

Monitoring acute metabolic changes in the liver and kidneys induced by fructose and glucose using hyperpolarized [2-^{13}C]dihydroxyacetone

Irene Marco-Rius[1], **Cornelius von Morze**[1], **Renuka Sriram**[1], **Peng Cao**[1], **Gene-Yuan Chang**[2], **Eugene Milshteyn**[1], **Robert A. Bok**[1], **Michael A. Ohliger**[1], **David Pearce**[2], **John Kurhanewicz**[1], **Peder E. Z. Larson**[1], **Daniel B. Vigneron**[1], and **Matthew Merritt**[3,4]

[1] Department of Radiology and Biomedical Imaging, University of California San Francisco, San Francisco, California

[2] Department of Medicine, Division of Nephrology, University of California San Francisco, San Francisco, California

[3] Department of Biochemistry and Molecular Biology, University of Florida, Gainesville, Florida

Abstract

Purpose—To investigate acute changes in glucose metabolism in liver and kidneys in vivo after a bolus injection of either fructose or glucose, using hyperpolarized [2-^{13}C]dihydroxyacetone.

Methods—Spatially registered, dynamic, multi-slice MRS were acquired for the metabolic products of [2-^{13}C]dihydroxyacetone in liver and kidneys. Metabolism was probed in 13 fasted rats at three time points: 0, 70 and 140 minutes. At 60 minutes, rats were injected intravenously with fructose (n=5) or glucose (n=4) at 0.8 g/kg to initiate acute response. Controls (n=4) did not receive a carbohydrate challenge.

Results—Ten minutes after fructose infusion, levels of [2-^{13}C]phosphoenolpyruvate and [2-^{13}C]glycerol-3-phosphate halved in liver: 51% (P=0.0010) and 47% (P=0.0001) of baseline, respectively. Seventy minutes later, levels returned to baseline. The glucose challenge did not alter the signals significantly, nor did repeated administration of the dihydroxyacetone imaging bolus. In kidneys, no statistically significant changes were detected after sugar infusion other than a 20% increase of the glycerol-3-phosphate signal between 10 and 80 minutes after fructose injection (P=0.0028).

Conclusion—Hyperpolarized [2-^{13}C]dihydroxyacetone detects a real-time, transient metabolic response of the liver to an acute fructose challenge. Observed effects possibly include ATP depletion and changes in the unlabeled pool sizes of glycolytic intermediates.

Keywords

dynamic nuclear polarization; hyperpolarization; metabolic imaging; gluconeogenesis; glycolysis; glycerol-3-phosphate; phosphoenolpyruvate

[4] Corresponding author: Matthew Merritt, matthewmerritt@ufl.edu.

INTRODUCTION

Gluconeogenesis (GNG) in the liver and to a lesser extent the kidney is integrally associated with whole body glucose homeostasis [1,2]. This process is poorly controlled in diabetes, and it is now recognized that GNG is dysregulated in non-alcoholic fatty liver disease (NAFLD) [3], which has prevalence of 80-90% in obese adults [4]. NAFLD can progress to non-alcoholic steatohepatitis (NASH), which is projected to be the primary cause for liver transplantation within the next decade [5]. GNG is likewise known to be disrupted in cirrhosis [3], which results from progressive fibrotic liver injury. Invasive liver biopsy, despite its associated complications with bleeding and mortality, remains the primary method of monitoring the progression of NAFLD to NASH [6] or staging liver fibrosis [7]. The development of improved methodology for non-invasive diagnosis and monitoring of these conditions represents an extremely important unmet clinical need in hepatology.

The highly prevalent fructose-rich diet promotes liver injury. High-fructose diets have been shown to increase insulin resistance, hypertension, lipid synthesis, obesity and metabolic syndrome [8]. It is believed that fructose toxicity is primarily related to its unregulated uptake and subsequent hepatic ATP depletion [9]. The strong association of diet composition with NAFLD as well as progression to NASH indicates that derangement of energy metabolism underlies disease pathogenesis, with fructose metabolism playing a key role [6].

The acute response to a fructose insult may provide valuable information on metabolic status of liver and kidneys. Recently, a metabolic challenge using fructose has been used to assay ATP availability in the liver [10]. The fructose challenge manifested changes in ^{31}P spectroscopy studies, with subjects that consumed a high level of dietary fructose reflecting lower ATP/inorganic phosphate ratio than subjects that consumed less. Fewer studies have investigated the impact of fructose on energy metabolism in the kidney [11]. Given the strong known association of diabetes and hypertension (exemplified in the metabolic syndrome), the impact could be significant and therefore fructose metabolism in the kidney warrants further study as well.

Hyperpolarized (HP) ^{13}C MRI is a new method for investigating local tissue metabolism non-invasively, based on >10,000-fold signal enhancement [12] compared to conventional ^{13}C NMR. HP [1-^{13}C]pyruvate MRI was recently applied for first-in-man studies of cancer metabolism [13]. New preclinical studies have demonstrated the feasibility of probing gluconeogenic pathways using HP [2-^{13}C]dihydroxyacetone (DHAc) [14,15]. DHAc has superior properties for imaging GNG/glycolysis compared to pyruvate, as it enters the Embden-Meyerhof pathway at dihydroxyacetone phosphate (DHAP) (Fig. 1), sidestepping the rate limiting enzyme phosphoenolpyruvate carboxykinase (PEPCK). DHAc metabolism should be responsive to changes in the Embden-Meyerhof pathway induced by fructose. Furthermore, DHAc shares with pyruvate the favorable properties of long T_1 relaxation time (resulting in long signal lifetime) and rapid metabolism into multiple distinct metabolic fates (providing rich metabolic data). Here, a spectrally selective imaging protocol [14] was used to image HP DHAc metabolism in the kidney and liver after an intravenous fructose challenge. The goal of this study was to investigate the effects of fructose vs. glucose challenge, as

compared with controls, on metabolic status in the liver and kidneys using HP [2-^{13}C]DHAc.

METHODS

Hyperpolarization of [2-^{13}C]dihydroxyacetone

A stock solution of [2-^{13}C]DHAc was prepared as in Marco-Rius *et al.* 2016 [14]. Briefly, a sample containing 8 M [2-^{13}C]DHAc, 21 mM trityl radical OX063 (Oxford Instruments, Abingdon, UK), and 1.0 mM gadolinium-DOTA chelate dissolved in 2:1 water:DMSO was polarized using an Oxford HyperSense polarizer operating at 3.35 T and 1.3 K. The frozen sample was then dissolved in a superheated solution of phosphate-buffered saline to obtain a final concentration of 80 mM of [2-^{13}C]DHAc with neutral pH.

Animal preparation

All animal studies were carried out under a protocol approved by the University of California San Francisco (UCSF) Institutional Animal Care and Use Committee.

The concentration of glucose in the blood was measured immediately prior to the first DHAc injection and every 10-20 minutes after that using a glucometer (Contour, Bayer Corporation, Parsippany, NJ, US). A drop of blood was collected by pricking the end of the tail for every glucose reading. Glucose blood level measurements were corrected for the added blood volume due to injections in the rat, assuming an initial blood volume of 13.5 ml for every 0.25 kg of body weight [16], which increased by ~2.7 ml after each DHAc injection and by ~0.7 ml after the fructose or glucose infusion.

Glucose and fructose loading effects probed with [2-^{13}C]dihydroxyacetone— Thirteen Sprague Dawley rats (age = 4-6 months, weight = 0.4-0.5 kg) were fasted for 20-24 hours with ad libitum water access, and anesthetized immediately prior to the MRS experiments by administration of inhalational isoflurane via nose cone (3.5% isoflurane/ oxygen mixture for induction, gas flow rate 1 l/min). A tail-vein cannula was inserted, and its patency maintained with heparin diluted in sterile saline (4 U/ml). The animal was placed on a warm pad inside a dual-tuned birdcage coil to maintain its body temperature at 37°C and isoflurane delivery was kept at 1.5-1.7% (1 l/min) throughout the experiment. During each experimental session, all animals underwent multi-slice HP [2-^{13}C]DHAc MRS scans at three time points (except one control that received only the first two): 0 (baseline), 70, and 140 minutes after baseline. Five animals received an intravenous bolus of 0.8 g/kg of fructose in phosphate buffer (0.5 g/ml, neutral pH) 60 minutes after the first DHAc injection (10 minutes prior to the second DHAc injection), 4/13 were given an intravenous bolus of 0.8 g/kg of glucose in phosphate buffer (0.5 g/ml, neutral pH) 60 minutes after the first DHAc injection (10 minutes prior to the second DHAc injection), and 4/13 were used as controls (did not receive any glucose or fructose but received 3 doses of DHAc).

Acquisition details of hyperpolarized MR studies in vivo

MRS experiments were performed using a 3T clinical MRI system (MR 750, GE Healthcare, Waukesha, WI, USA) equipped with 50 mT/m, 200 mT/m/ms gradients and a

broadband RF amplifier. ^{1}H and ^{13}C RF transmission and signal reception was performed with a custom-built, dual-tuned rat birdcage coil.

^{1}H images were acquired for anatomic reference using a 3D balanced steady-state free precession (bSSFP) sequence (0.6mm isotropic resolution, TE = 2.2 ms, TR = 5.3 ms). ^{13}C RF power and center frequency calibration were performed using a 1 ml vial filled with 6.0 M ^{13}C-urea placed on the rat abdomen in the coil.

Hyperpolarized [2-^{13}C]DHAc was injected into the tail vein of a rat over 12 s (2.7 ml, 80 mM solution, <20 s after dissolution). Dynamic ^{13}C MRS acquisition started 15 s after the beginning of the injection.

Two adjacent axial slabs of 1 cm thickness centered on the liver and kidneys, respectively, were excited in a dynamic, alternating manner using a five-band spectral-spatial RF pulse centered on a urea phantom resonance (δ_{urea} = 163.2 ppm). The inter-slice spacing was 15-20 mm, depending on rat anatomy (Fig. 2). There was a temporal delay of 1.5 s between the liver and kidney acquisitions. Additional acquisition parameters included: TR for dynamic acquisition = 3 s; receiver bandwidth = 10 kHz; number of points = 2048; flip angle = 0.3° at the DHAc resonance ($\delta_{C2\text{-}DHAc}$ = 213 ppm), 26° at the phosphoenolpyruvate (PEP) resonance ($\delta_{C2\text{-}PEP}$ = 151 ppm), 2.3° at the DHAc hydrate resonance ($\delta_{C2\text{-}hydr}$ = 96 ppm), 20° at an additional resonance at 88 ppm, and 20° at the glycerol 3-phosphate (G3P) resonance ($\delta_{C2\text{-}G3P}$ = 73 ppm).

Data processing and T_1 calculation

Data were processed using Matlab (Mathworks, Natick, MA). Prior to Fourier transformation, raw data were truncated to 1000 points, a 10 Hz line broadening was applied, and data were zero-filled to 4000 points. The spectral baseline offset was corrected by calculating the mean intensity of the noise (400 points on the edge of each spectrum) and subtracting it from all of the points in the spectrum.

The areas under the metabolic peaks of interest (magnitude spectra) were measured to obtain a time-course of the signal decay. Integral limits were defined for liver and kidney spectra separately. The same integral limits were used across the three spectra of the same organ acquired in the same experimental session. Figure 4 displays the results after summing the integral values of the first 10 acquisitions, normalized to the DHAc hydrate sum in the same slab. This ratiometric approach of normalizing to the hydrate was selected in order to minimize variations due to several factors, including substrate polarization, concentration, volume of infusion, tracer delivery, and coil loading and placement.

To calculate the apparent T_1's of the metabolic products of DHAc in vivo, the integrals of the resonances of the metabolic products of HP DHAc were corrected for the applied flip angle and an exponential decay was fitted to the time-course of the corrected integrals. A summary of the apparent T_1 results are presented in Table 1.

Statistical analysis

All results are expressed as mean ± standard deviation. Statistical significance of the results was determined calculating a two-way, repeated-measurement ANOVA with Tukey's multiple comparison test in Prism 7 (GraphPad Inc., La Jolla, CA). Performing one ANOVA test for each metabolite and organ, the test accounted for the three groups and the repeated, matched measurements. One control rat that received only two DHAc injections was excluded from the statistical analysis. An adjusted P-value < 0.0167 (Bonferroni correction for 3 ANOVA tests [17]) was considered significant (0.001 < P < 0.0167 was indicated with *, and P < 0.001 was indicated with **).

RESULTS

Characterization of the MRS spectra of hyperpolarized [2-^{13}C]dihydroxyacetone

To assign the resonances produced through the metabolism of [2-^{13}C]DHAc in vivo, an initial ^{13}C MRS acquisition was performed on a syringe containing HP DHAc solution. The liquid state HP [2-^{13}C]DHAc solution was found to attain a polarization level of 15% upon dissolution after a buildup of 70 minutes (buildup time constant τ = 1080s). Following in vivo administration of HP DHAc via tail vein injection, the resonances corresponding to DHAc ($\delta_{C2\text{-}DHAc}$ = 213.4 ppm) and DHAc hydrate ($\delta_{C2\text{-}hydr}$ = 96.5 ppm) were observed, as well as resonances originating from unknown impurities in the sample. Additionally, three metabolic products of HP DHAc were observed at distinct resonances: [2-^{13}C]glycerol-3-phosphate (G3P) as a doublet ($\delta_{C2\text{-}G3P}$ = 75.0 and 70.4 ppm, $J_{CH} \approx$ 147 Hz), [2-^{13}C]glyceraldehyde-3-phosphate (GA3P) in between the G3P doublet ($\delta_{C2\text{-}Ga3P}$ = 73.8 ppm), and [2-^{13}C]PEP ($\delta_{C2\text{-}PEP}$ = 151.1 ppm) (Fig. 3). Since the G3P doublet was much larger than the GA3P signal, they were integrated together, and throughout we will use G3P to refer to the area including both metabolites.

The lifetime of HP DHAc at 3T was sufficiently long to be used as a substrate to study metabolism (T_1 = 39 s in solution, 20 s in vivo – estimated from a separate acquisition using a conventional slice-selective sinc RF pulse centered on the DHAc resonance). Table 1 shows the apparent T_1 relaxation times of G3P and DHAc hydrate in vivo, which were determined by fitting an exponential decay function to the time curve of the integrals of the resonances of the metabolic products of HP DHAc (corrected for the applied flip angle). The apparent T_1s of G3P (~30s) and DHAc hydrate (~17s) were the same in the kidneys and in the liver. The signal intensity of PEP was too low to determine the T_1 accurately. Based on the disappearance of the PEP signal after 3-4 acquisitions (~25 s after the beginning of the injection), the estimated apparent T_1 of PEP was ~5-10 s in vivo. Since there were no differences among repeated HP DHAc injections, apparent T_1 data of the metabolites is presented as one value (n=39).

An example of the timecourse of the integrals for liver and kidneys is shown in figure 5.

Assessment of the metabolic effects of hyperpolarized [2-^{13}C]dihydroxyacetone

To test whether the repeated injection of HP DHAc produced any metabolic changes, a control group (n=4) received three injections of HP DHAc alone, each 70 minutes apart (except one control rat that received only the first two injections).

Glucometer readings in figure 4a (black circle) taken every 10-20 minutes indicate that repeated injections of 80 mM HP DHAc solution did not induce detectable changes in blood glucose levels (there was a ± 30 mg/dl intrinsic variability of the glucometer readings).

Also, in the control group no metabolic changes were detected by ^{13}C-MRS when probed with DHAc, i.e. the ratios G3P/DHAc hydrate and PEP/DHAc hydrate in liver (Fig. 4b) and kidneys (Fig. 4c) did not change significantly across the three injections.

Glucose loading effects on metabolism probed with [2-^{13}C]dihydroxyacetone

Four Sprague Dawley rats received an intravenous bolus of glucose solution (0.8 g/kg) 60 minutes after the first HP DHAc injection (i.e. baseline), and their metabolism was probed with two additional HP DHAc injections at 70 and 140 minutes after baseline.

The glucose concentration in blood increased immediately after glucose administration, surpassing 300 mg/dl seven minutes after glucose infusion. A maximum of (328 ± 45) mg/dl (n=4) was reached ~20 minutes after glucose infusion, which is ~3 times the baseline level (Fig. 4a, blue square). Despite this increase in the blood glucose level, no metabolic changes were detected by probing the metabolism of liver and kidneys with DHAc, i.e. the integral of the G3P and PEP resonances remained at baseline levels. Eighty minutes after glucose infusion, blood glucose levels had dropped to just ~30% higher than baseline, and the DHAc spectra showed no differences with the previous two ^{13}C-MRS acquisitions (Fig. 3b, Fig. 4b, Fig. 4c).

Fructose loading effects on metabolism probed with [2-^{13}C]dihydroxyacetone

A bolus of fructose given at the same dose as glucose, (0.8 g/kg), also produced an increase in the blood glucose level, albeit the maximum [(212 ± 30) mg/dl, n=4] was only ~ 1.8 times larger than the baseline blood glucose value (Fig. 4a, red triangle). For the first 10 minutes post-fructose infusion, the glucose concentration in blood remained close to baseline levels. The increase was noticeable about 20 minutes after the fructose injection, while the maximum level was reached 30-40 minutes after administration of fructose.

Ten minutes after fructose infusion blood glucose levels had not departed from baseline. However, the integral of the G3P and PEP metabolic peaks in the liver decreased with respect to baseline by 47% (P=0.0001) and 51% (P=0.0010), respectively (Fig. 3c, Fig. 4b, Fig. 4c). In the kidneys, the slight decrease of the G3P integral measured was not significant (11%, P=0.0731).

Seventy minutes later (third HP DHAc injection), both blood glucose levels and resonances had returned to baseline. No statistical significance was found between baseline and 140 minutes later in any of the groups. The integrals of the G3P and PEP in the liver increased significantly with respect to the ten minutes time point (second HP DHAc injection) by

150% (P=0.00002) and 109% (P=0.0039), respectively (Fig. 3c, Sup. Fig. S2, Sup. Fig. S3). In the kidneys, there was a significant 28% increase of the G3P signal (P=0.0028).

DISCUSSION

Hyperpolarized [2-^{13}C]dihydroxyacetone as a metabolic imaging agent

Our results demonstrate the feasibility of using HP DHAc to assess gluconeogenic metabolism and ATP availability in the liver and in the kidneys non-invasively, which could potentially alter patient care standards, minimizing patient pain and discomfort associated with biopsies (particularly in patients with clotting problems due to liver dysfunction) and enabling longitudinal studies of disease progression or the effects of treatment [6].

We have shown that HP DHAc satisfies key requirements for HP metabolic imaging, including high polarization (~15%, providing a 50,000-fold increase in detection sensitivity at 3T), and sufficiently long T_1 of DHAc and its downstream metabolites to acquire kinetic data in vivo (Fig. 5, Table 1). Moreover, the uptake and metabolism of DHAc is on the timescale of T_1. DHAc enters the glycolytic/gluconeogenic pathway at the DHAP level (Fig. 1), and it has previously been shown that in perfused liver it is rapidly metabolized into upstream and downstream metabolites [15]. Our results in vivo indicated that liver but not kidney is the primary site of DHAc metabolism. Here, MRS signal localization is limited to 1-cm slabs. The “liver slab” comprises mainly the liver, with traces of stomach, spleen and vasculature. The kidneys are the metabolically-active organs enclosed in the “kidney slabs”, but the circulating HP substrate in the aorta contributes to the HP DHAc and hydrate signal. Since the kidney slab produces a larger HP DHAc hydrate signal than the liver, and perfusion and metabolic uptake is different in each organ, the acute changes in the metabolites ratios at the three time-points are compared for liver and kidneys independently. While the precise mechanism of DHAc transport is not known, its entry into the hepatic Embden-Meyerhof pathway is rapid as evidenced by the downstream metabolites observed. DHAc kinase produces DHAP from DHAc, and has an activity of 0.71 units/mg protein in the rat liver [18]. Similar activities for the kinase are expected in the kidney [19]. Since the amplitudes of downstream DHAc metabolites in the kidney are notably decreased as compared to the liver (Fig. 3), we surmise that transport of DHAc into kidney is restricted on the timescale of the MR experiment. Also, the higher hepatic metabolism of fructose is evidenced by the muted effect of the fructose challenge in the kidney as compared to the liver [20] (Fig. 4b and c). The origin of the resonance at ~89 ppm has not been identified. Since we did not detect this peak in solution, it is possible that it arose from metabolic conversion, but is currently unidentified.

The results indicate that DHAc produces minimal interference of the metabolic pathway of interest. Our study design included multiple injections of DHAc to assess the serial effects of the substrate administration on glucose homeostasis [21]. Figure 4a and supporting figure S1 demonstrate that the quantity of DHAc used for metabolic imaging does not perturb circulating glucose levels.

Glucose Challenge

Intravenous glucose was administered after a fast of 24 h, when the rat liver would be expected to be in a gluconeogenic regime with little stored glycogen remaining [22]. Circulating glucose is transported into liver cells by Glut2, where glucokinase phosphorylates glucose and prevents its export [2]. Despite ATP utilization by this process, the glucose challenge failed to produce significant changes in any of the measured variables (Fig. 4, Sup. Fig. S2, Sup. Fig. S3). Because of the tight metabolic regulation associated with glucokinase, it is highly likely that hepatic glucose uptake was well controlled, and therefore glycolysis/GNG was largely unperturbed. Additionally, it has been reported that the glucose regulatory system of rats is less responsive to an increase in the circulating glucose than other animal species [23]. The lack of variability in the measured parameters using the glucose challenge serves as an excellent control for the fructose challenge.

A recent study reports a large change on HP pyruvate metabolism by the kidney due to acute sucrose ingestion [24]. The oral glucose tolerance test has some important biological differences compared to the intravenous glucose challenge. An equivalent quantity of intragastric glucose, as in normal meal ingestion, is associated with a much larger insulin response, via the incretin effect [25], i.e. gut-specific glucose sensors that stimulate insulin secretion from the pancreatic beta-cells are by-passed when glucose is injected intravenously. Furthermore, ingested glucose is delivered to the liver first via the portal vein, while intravenously-injected glucose is distributed in the systemic circulation, reaching heart, brain, lungs and kidneys before being delivered to the liver [26].

Fructose challenge

The metabolism of fructose is well-known for its highly gluconeogenic nature [21], but it is also connected to glycolysis, glycogen synthesis, and lipogenesis [20,27] (Fig. 1). A high-fructose diet, for example, induces long term changes in ATP availability and enzyme activities [10]. The rats used here were fed on normal chow, and therefore any metabolic changes detected with our method result solely from the acute effect of the bolus of fructose injected.

The infusion of fructose, which is also transported into the cells by Glut2, results in accumulation of fructose 1-phosphate (F1P) due to a high fructokinase activity, low aldolase B activity, and a shifted equilibrium constant towards F1P [28]. The conversion of fructose to F1P depletes the liver of ATP as the process is not strongly regulated, and the inorganic phosphate pool needed for phosphorylation of ADP is challenged [28,29]. This perturbation of the energy homeostasis triggers several biochemical reactions, such as the inhibition of phosphorylase *a* and enhanced glycogen production [30]. The two trioses resulting from the metabolism of F1P (DHAP and glyceraldehyde) can be further metabolized to enter the gluconeogenic/glycolytic/glycogen synthesis pathway (via GA3P) or the lipid synthesis pathway (via G3P) (Fig. 1).

The fructose challenge produced significant drops (even with Bonferroni correction) in the liver PEP and G3P resonances (Fig. 4b, Sup. Fig. S2a, Sup. Fig. S3a) prior to any changes in the circulating glucose concentration (Fig. 4a) while kidney PEP and G3P remained

unperturbed (Fig. 4c, Sup. Fig. S2b, Sup. Fig. S3b). Seventy minutes later, the G3P and PEP integrals had return to baseline levels. In the kidneys, G3P integral changed significantly between the second and third DHAc shots. However, the lack of a significant difference between time-points 1 and 3, and between time-points 1 and 2, corroborate that the difference between points 2 and 3 was not indicative of an important change in biology following injection of fructose. This agrees well with the fact that fructose is mainly metabolized in the liver [27]. A decrease of the observed hepatic PEP and G3P may be explained by the decrease in ATP availability immediately after the fructose injection, which inhibits the phosphorylation of DHAc. Additionally, it had been previously reported that DHAP concentration in liver increases 10 minutes after fructose administration (in continuous infusion in perfused liver [29] and after a bolus injection via tail vein in rats in vivo [28]). In the context of our HP experiments, this may translate into an increase of the unlabeled pool of DHAP and a consequent decrease in carbon-13 labeled G3P and PEP production from the exogenous HP ^{13}C-DHAc. These experiments at 3T, like prior experiments in perfused liver at 9.4T [15], were not able to distinguish the DHAP resonance from DHAc. Since the high HP DHAc signal would mask any changes in DHAP and no additional information would be extracted from this resonance, a spectral-spatial pulse was used to minimize excitation of DHAc (and DHAP) and preserve magnetization of the metabolites beyond DHAP.

While changes in individual metabolites were significant, the ratio of G3P/PEP was not particularly sensitive to any protocol used here. Although this is in apparent contradiction to previous work [15], a closer analysis of fructose metabolism provides a possible explanation. While fructose is highly gluconeogenic, it does not drive GNG from 3-carbon metabolism and the TCA cycle. Given that it consumes phosphate moieties in its initial metabolism to F1P and drives 3-carbon intermediate pool sizes, changes in DHAc metabolism would most likely manifest in the 6-carbon intermediates of the Embden-Meyerhof pathway. Unfortunately, with the sensitivity achieved, these intermediates were not detected using the current protocol. Future experiments could be enhanced by using proton decoupling or higher field DNP polarizers that produce commensurate increases in the signal enhancement.

CONCLUSIONS

We have demonstrated that DHAc metabolism is responsive to fructose challenge. Because DHAc enters the glucose metabolism at the intermediate triose phosphate level, in the vicinity of fructose, it is ideally suited for assessing changes in aberrant glucose or glycerol metabolism. This observation is complementary to prior ^{31}P NMR studies in humans [10]. DHAc may probe alterations in hepatic energy homeostasis or key enzyme activities (such as G3P dehydrogenase) occurring in diabetes[31], NASH [32], obesity[10,33,34] or cirrhosis [35], in a non-invasive manner. The clinical translational potential of this probe benefits from an exceptional safety profile, having been given as an oral metabolic challenge nearly a century ago [36]. Future work is proceeding along these lines.

Supplementary Material

Refer to Web version on PubMed Central for supplementary material.

ACKNOWLEDGEMENTS

We thank Dr. I. E. Allen from the Epidemiology and Biostatistics Department (UCSF) for advice on the statistical analysis. This work was supported by an intramural UCSF radiology department seed grant, and NIH grants P41EB013598, P41EB015908, R21EB016197, and R37HL34557. CVM was supported by NIH K01DK099451. This publication was supported by the National Center for Advancing Translational Sciences, National Institutes of Health, through UCSF-CTSI Grant Number UL 1 TR991872. Its contents are solely the responsibility of the authors and do not necessarily represent the official views of the NIH.

REFERENCES

1. Gerich J, Meyer C, Woerle H, Stumvoll M. Renal gluconeogenesis. Its importance in human glucose homeostasis. Diabetes Care. 2001; 24(2):382–391. [PubMed: 11213896]
2. Pilkis SJ, Granner DK. Molecular physiology of the regulation of hepatic gluconeogenesis and glycolysis. Annu Rev Physiol. 1992; 54(1):885–909. [PubMed: 1562196]
3. Sunny N, Parks E, Browning J, Burgess S. Excessive hepatic mitochondrial TCA cycle and gluconeogenesis in humans with nonalcoholic fatty liver disease. Cell Metab. 2011; 14(6):804–810. [PubMed: 22152305]
4. Bellentani S, Scaglioni F, Marino M, Bedogni G. Epidemiology of non-alcoholic fatty liver disease. Dig Dis. 2010; 28(1):155–161. [PubMed: 20460905]
5. Mahady SE, George J. Management of nonalcoholic steatohepatitis. An evidence-based approach. Clin Liver Dis. 2012; 16(3):631–645. [PubMed: 22824485]
6. Wree A, Broderick L, Canbay A, Hoffman HM, Feldstein AE. From NAFLD to NASH to cirrhosis-new insights into disease mechanisms. Nat Rev Gastroenterol Hepatol. 2013; 10(11):627–36. [PubMed: 23958599]
7. Varenika V, Fu Y, Maher JJ, Gao D, Kakar S, Cabarrus MC, Yeh BM. Hepatic fibrosis: evaluation with semiquantitative contrast-enhanced CT. Radiology. 2013; 266(1):151–8. [PubMed: 23169796]
8. Rutledge AC, Adeli K. Fructose and the metabolic syndrome?: pathophysiology and molecular mechanisms. Nutrition. 2007; 65(6):13–23.
9. van den Berghe G, Bronfman M, Vanneste R, Hers HG. The mechanism of adenosine triphosphate depletion in the liver after a load of fructose. A kinetic study of liver adenylate deaminase. Biochem J. 1977; 162(3):601–9. [PubMed: 869906]
10. Abdelmalek MF, Lazo M, Horska A, Bonekamp S, Lipkin EW, Balasubramanyam A, Bantle JP, Johnson RJ, Diehl AM, Clark JM. Higher dietary fructose is associated with impaired hepatic adenosine triphosphate homeostasis in obese individuals with type 2 diabetes. Hepatology. 2012; 56(3):952–960. [PubMed: 22467259]
11. Johnson RJ, Sanchez-Lozada LG, Nakagawa T. The effect of fructose on renal biology and disease. J Am Soc Nephrol. 2010; 21(12):2036–2039. [PubMed: 21115612]
12. Ardenkjaer-Larsen JH, Fridlund B, Gram A, Hansson G, Hansson L, Lerche MH, Servin R, Thaning M, Golman K. Increase in signal-to-noise ratio of >10,000 times in liquid-state NMR. Proc. Natl. Acad. Sci. USA. 2003; 100(18):10158–10163. [PubMed: 12930897]
13. Nelson SJ, Kurhanewicz J, Vigneron DB, Larson PEZ, Harzstark AL, Ferrone M, van Criekinge M, Chang JW, Bok R, Park I, et al. Metabolic imaging of patients with prostate cancer using hyperpolarized [1-^{13}C]pyruvate. Sci Transl Med. 2013; 5(198):198ra108. [accessed 2014 Sep 30]. http://www.ncbi.nlm.nih.gov/pubmed/23946197.
14. Marco-Rius I, Cao P, von Morze C, Merritt M, Moreno KX, Chang G-Y, Ohliger M a. Pearce D, Kurhanewicz J, Larson PEZ, et al. Multiband spectral-spatial RF excitation for hyperpolarized [2-13 C]dihydroxyacetone 13 C-MR metabolism studies. Magn Reson Med. 2016
15. Moreno KX, Satapati S, DeBerardinis RJ, Burgess SC, Malloy CR, Merritt ME. Real-time detection of hepatic gluconeogenic and glycogenolytic states using hyperpolarized [2-13C]dihydroxyacetone. J Biol Chem. 2014; 289:35859–35867. [PubMed: 25352600]
16. Davies B, Davies B, Morris T, Morris T. Physiological parameters in laboratory animals and humans. Pharmaceut Res. 1993; 10(7):1093.
17. McDonald, JH. Handbook of biological statistics. Sparky House Publishing; Baltimore, Maryland, USA: 2008.

18. Tsao MU, Teagan SJ, Borondy PE, Hogg JF. Metabolism of dihydroxyacetone in rat liver preparations. Metabolism. 1965; 14(3):246–252. [PubMed: 14261409]
19. Burch HB, Lowry OH, Meinhardt L, Max P, Chyu K. Effect of fructose, dihydroxyacetone, glycerol, and glucose on metabolites and related compounds in liver and kidney. J Biol Chem. 1970; 245(8):2092–2102. [PubMed: 5443994]
20. Mayes PA. Intermediary metabolism of fructose. Am J Clinical Nutrition. 1993; 58(suppl):754S–65S. [PubMed: 8213607]
21. Ross BD, Hems R, Krebs HA. The rate of gluconeogenesis from various precursors in the perfused rat liver. Biochem J. 1967; 102(3):942–51. [PubMed: 16742514]
22. Nowland MH, Hugunin KMS, Rogers KL. Effects of short-term fasting in male Sprague-Dawley rats. Comp Med. 2011; 61(2):138–44. [PubMed: 21535924]
23. Sacca L, Perez G, Rengo F, Critelli G. Some peculiarities of the glucoregulatory response to glucose infusion in the rat. Acta Diabet. 1976; 13(1):1–7.
24. Laustsen C, Hansen ESS, Kjaergaard U, Bertelsen LB, Ringgaard S, Stødkilde-Jørgensen H. Acute porcine renal metabolic effect of endogastric soft drink administration assessed with hyperpolarized [1-13c]pyruvate. Magn Reson Med. 2015; 74(2):558–563. [PubMed: 26014387]
25. Nauck M, Stöckmann F, Ebert R, Creutzfeldt W. Reduced incretin effect in type 2 (non-insulin-dependent) diabetes. Diabetologia. 1986; 29(1986):46–52. [PubMed: 3514343]
26. McIntyre N, Turner DS, Holdsworth CD. The role of the portal circulation in glucose and fructose tolerance. Diabetologia. 1970; 6:593–596. [PubMed: 5494595]
27. Hallfrisch J. Metabolic effects of dietary fructose. FASEB J. 1990; 4(9):2652–60. [PubMed: 2189777]
28. Heinz F. Metabolism of fructose in liver. Acta Med Scand Suppl. 1972; 542:27–36. [PubMed: 4353468]
29. Woods HF, Eggleston L V, Krebs HA. The cause of hepatic accumulation of fructose 1-phosphate on fructose loading. Biochem. J. 1970; 119:501–510. [PubMed: 5500310]
30. Parniak MA, Kalant N. Enhancement of glycogen concentrations in primary cultures of rat hepatocytes exposed to glucose and fructose. Biochem J. 1988; 251(3):795–802. [PubMed: 3415647]
31. Szendroedi J, Chmelik M, Schmid AI, Nowotny P, Brehm A, Krssak M, Moser E, Roden M. Abnormal hepatic energy homeostasis in type 2 diabetes. Hepatology. 2009; 50(4):1079–1086. [PubMed: 19637187]
32. Cortez-Pinto H, Chatham J, Chacko VP, Arnold C, Rashid A, Diehl AM. Alterations in liver ATP homeostasis in human nonalcoholic steatohepatitis: a pilot study. J Am Med Assoc. 1999; 282(17): 1659–1664.
33. Nair S, Chacko VP, Arnold C, Diehl AM. Hepatic ATP reserve and efficiency of replenishing: Comparison between obese and nonobese normal individuals. Am J Gastroenerol. 2003; 98(2): 466–470.
34. Swierczynski J, Zabrocka L. Enhanced glycerol 3-phosphate dehydrogenase activity in adipose tissue of obese humans. Mol Cell Biochem. 2003; 254:55–59. [PubMed: 14674682]
35. Changani KK, Jalan R, Cox IJ, Ala-Korpela M, Bhakoo K, Taylor-Robinson SD, Bell JD. Evidence for altered hepatic gluconeogenesis in patients with cirrhosis using in vivo 31-phosphorus magnetic resonance spectroscopy. Gut. 2001; 49(4):557–64. [PubMed: 11559655]
36. Mason E, Hill E. Dihydroxyacetone studies I. Its respiratory and carbohydrate metabolism in normal men. J Clin Invest. 1926; 2(6):521–532. [PubMed: 16693698]

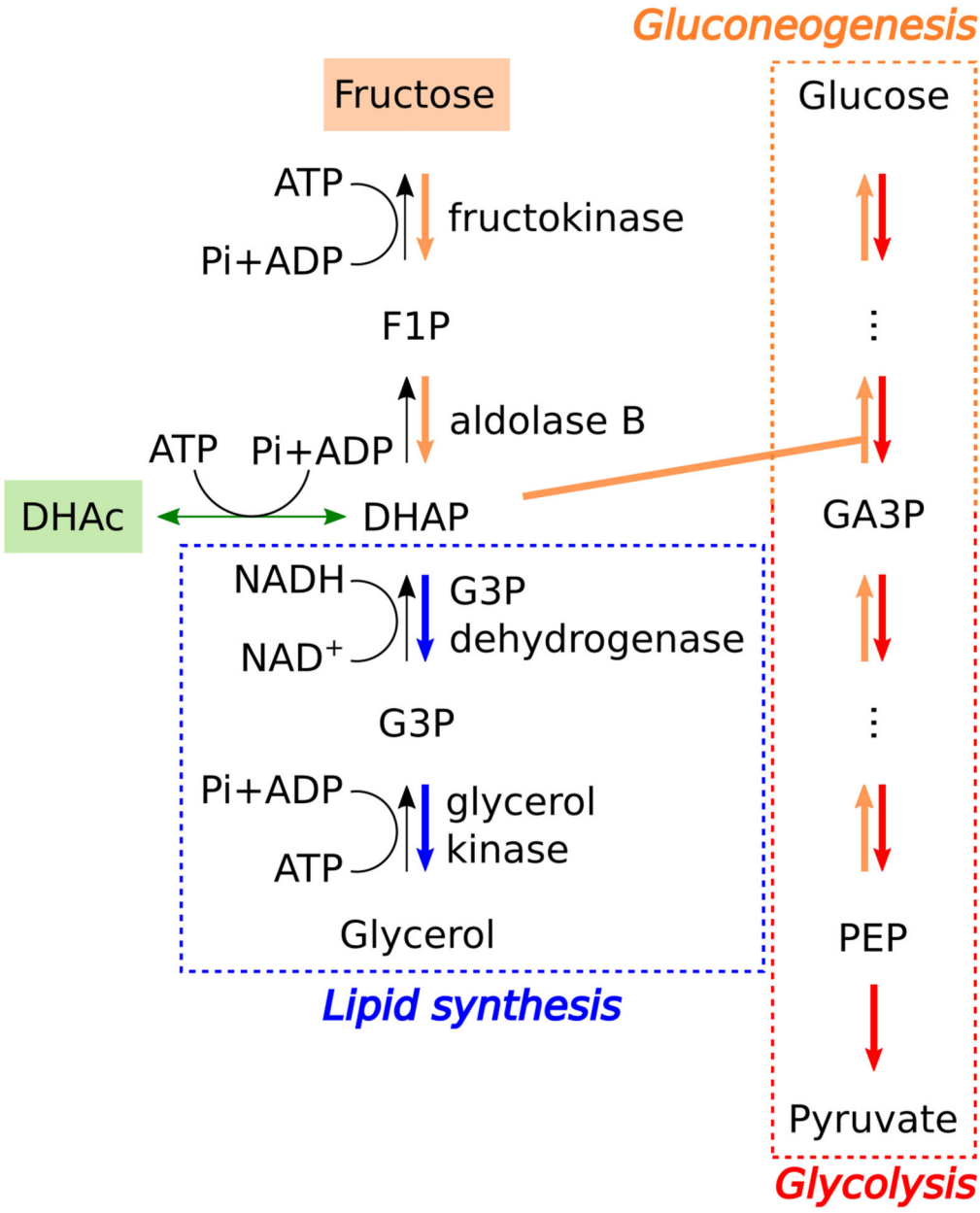

Figure 1.

Scheme of the metabolic fates of exogenously-injected fructose and hyperpolarized DHAc. DHAc = dihydroxyacetone, DHAP = dihydroxyacetone phosphate, F1P = fructose-1-phosphate, G3P = glycerol-3-phosphate, GA3P = glyceraldehyde-3-phosphate, PEP = phosphoenolpyruvate, hydr = DHAc hydrate.

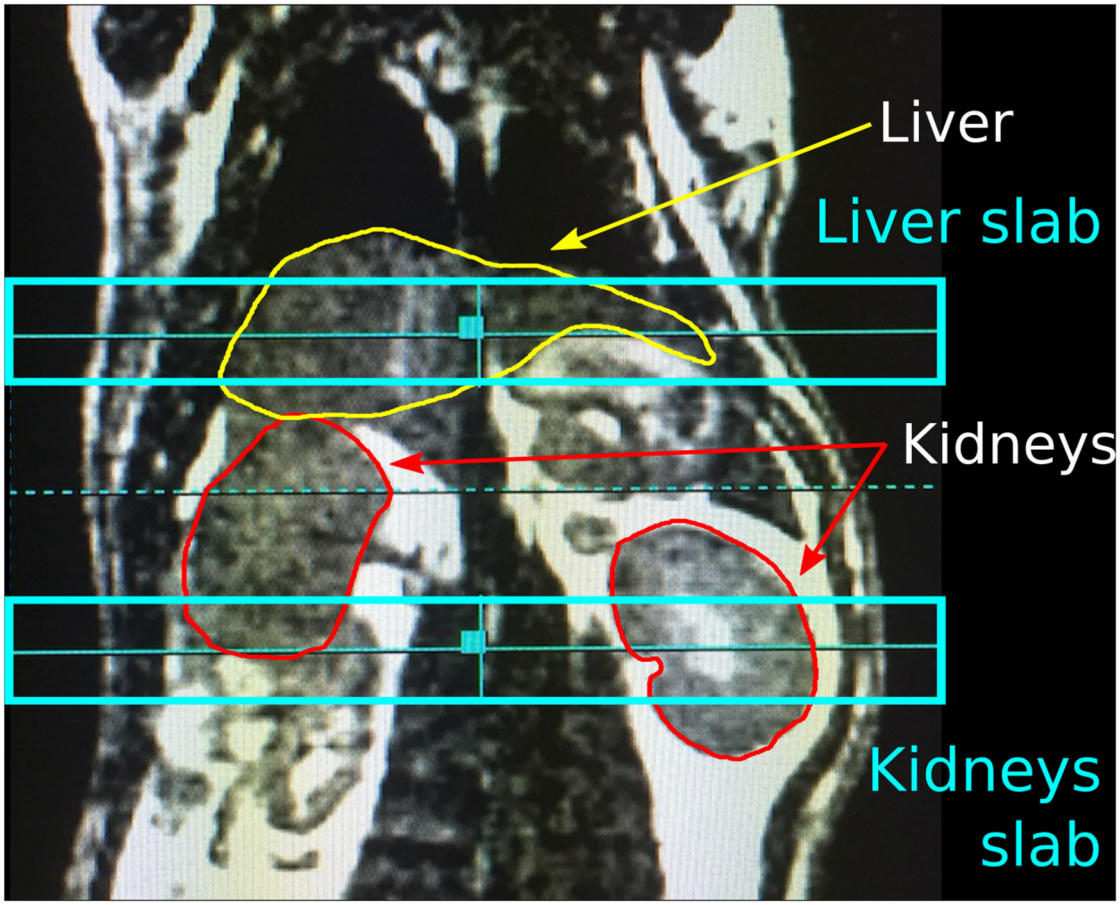

Figure 2.

Coronal anatomic reference showing the positioning of the 1-cm liver and kidney slabs and the contour of the liver (yellow) and kidneys (red). ^{1}H image was acquired using a 3D balanced steady-state free precession sequence.

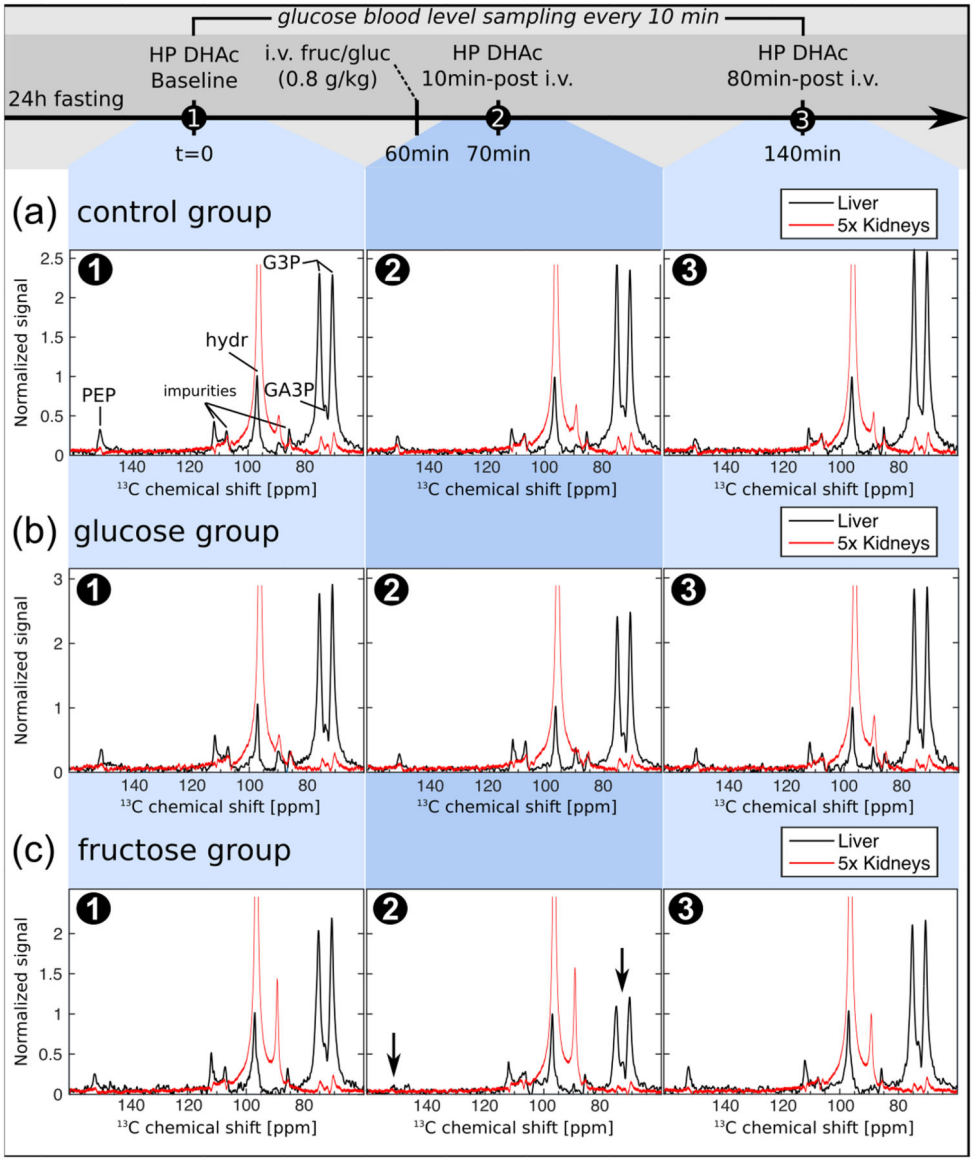

Figure 3.

Acute metabolic changes of the signal normalized to the signal DHAc hydrate detected in the liver (black line) and in the kidneys (red line, multiplied by a factor of five) in response to fructose load using hyperpolarized [2-^{13}C]DHAc MRS with spectral-spatial RF excitation. (a) ^{13}C-MR spectra of three injections of HP DHAc, each separated by 70 minutes in time. (b) As in (a), but with the additional bolus injection of a glucose solution (0.8 g/kg) ten minutes prior to the acquisition of the second DHAc spectra. (c) As in (a), but with the additional bolus injection of a fructose solution (0.8 g/kg) ten minutes prior to the acquisition of the second DHAc spectra. The concentration of glucose in blood was monitored every 10-20 minutes (Fig.4a). DHAc = dihydroxyacetone, G3P = glycerol-3-phosphate, PEP = phosphoenolpyruvate, hydr = DHAc hydrate.

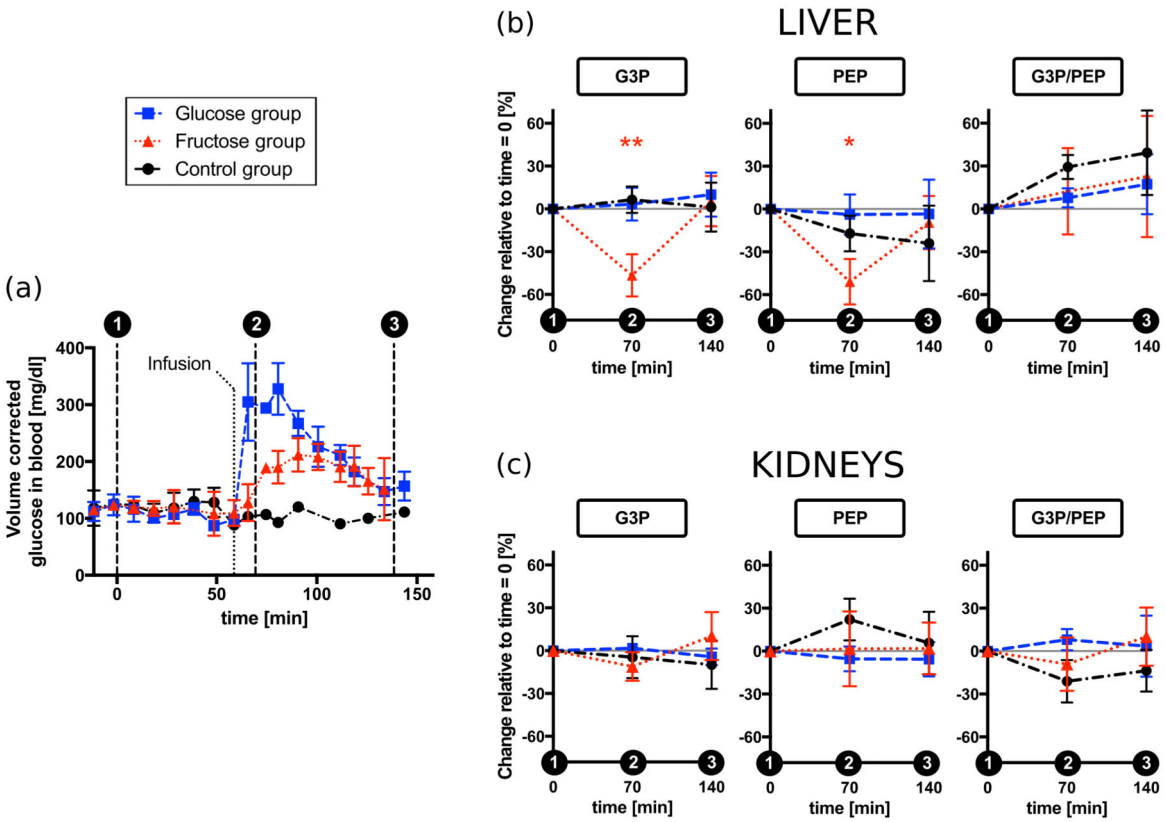

Figure 4.

Acute metabolic response of the liver and kidneys in vivo to fructose or glucose loading. (a) Time course of the glucose concentration in blood corrected for the increase in the total blood volume after each injection or infusion. Error bars show the standard deviation of the measurement across animals. The glucometer readings added a ± 30 mg/dl intrinsic variability not shown in this plot. (b) Liver results: Percentage change between the metabolites integrals at baseline and 10 minutes or 80 minutes after the carbohydrates infusion, which was administered 60 minutes after the baseline. (c) Kidneys results: Percentage change between the metabolites integrals at baseline and 10 minutes or 80 minutes after the carbohydrates infusion. Error bars correspond to the standard deviation of the mean. Statistical significance was only observed in the fructose group and indicated with one asterisk, *, ($0.001 < P < 0.0167$) or two, **, ($P < 0.001$). DHAc = dihydroxyacetone, G3P = glycerol-3-phosphate, PEP = phosphoenolpyruvate.

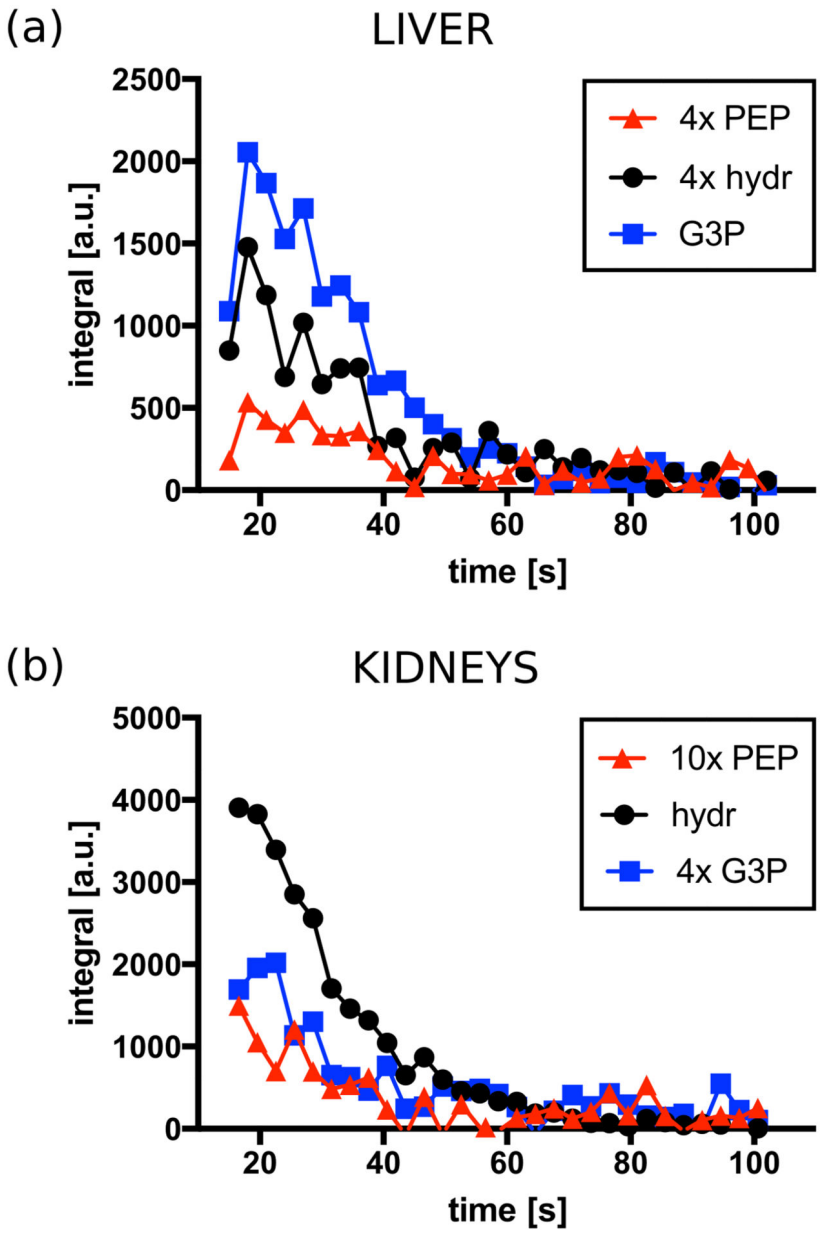

Figure 5.

Example of the time-course of the integrals of the PEP, G3P and DHAc hydrate resonances. DHAc = dihydroxyacetone, G3P = glycerol-3-phosphate, PEP = phosphoenolpyruvate, hydr = DHAc hydrate.

Table 1

Apparent T_1 relaxation times for the metabolic products of HP [2-^{13}C]DHAc in vivo. Data shown as mean ± standard deviation (n=39). The SNR of PEP was too low to determine T_1 accurately, but given that the PEP signal disappeared after the 3rd or 4th acquisitions, its T_1 was estimated to be ~5-10 s. DHAc = dihydroxyacetone, G3P = glycerol-3-phosphate, PEP = phosphoenolpyruvate.

T_1 G3P [s]		T_1 DHAc hydrate [s]	
Liver	**Kidney**	**Liver**	**Kidney**
31.2 ± 5.9	28.9 ± 8.9	17.3 ± 3.5	17.2 ± 1.3